Formation of toroidal bubbles from acoustic droplet vaporization

David S. Li,[1] Oliver D. Kripfgans,[2] Mario L. Fabiilli,[2] J. Brian Fowlkes,[2] and Joseph L. Bull[1]
[1]*Department of Biomedical Engineering, University of Michigan, Ann Arbor, Michigan 48109, USA*
[2]*Department of Radiology, University of Michigan, Ann Arbor, Michigan 48109, USA*

(Received 5 October 2013; accepted 23 January 2014; published online 13 February 2014)

Acoustic droplet vaporization (ADV) is the selective vaporization of liquid microdroplets using ultrasound to produce stable gas bubbles. ADV is the primary mechanism in an ultrasound based cancer therapy, called gas embolotherapy, where the resulting bubbles are used to create localized occlusions leading to tumor necrosis. In this investigation, early time scale events including phase change are directly visualized using ultra-high speed imaging. Modulating elevated acoustic pressure or pulse length resulted in toroidal bubbles. For sufficiently short pulses (4 cycles at 7.5 MHz), toroidal bubble formation could be avoided, regardless of acoustic pressures tested. © *2014 AIP Publishing LLC*. [http://dx.doi.org/10.1063/1.4864289]

Gas embolotherapy (GE) is a developmental ultrasound based cancer therapy.[1,2] The proposed treatment begins with the introduction of encapsulated liquid perfluorocarbon (PFC) microdroplets via intravenous injection. The PFC is chosen such that at body temperature (37 °C), the microdroplets may maintain a superheated liquid state depending on the size and stabilizing surface tension from the shell. Dodecafluoropetane (DDFP, C_5F_{12}) is a commonly used PFC for GE microdroplets with a bulk boiling point of 29 °C. DDFP microdroplets have been shown to remain in a stable liquid state even up to 65 °C as they do not spontaneously vaporize until a focused ultrasound pulse is applied.[3,4] After the liquid microdroplets are perturbed and vaporize, they undergo an expansion process to form stable gas bubbles that are approximately 125 times larger in volume than the initial droplets. The resulting bubbles can then lodge in the vasculature, diverting blood flow, and potentially causing tissue damage.[5,6] This method could be translated into a localized treatment of vascularized tumors. The mechanism in which liquid droplets are vaporized to form gas bubbles using an acoustic pulse can be described as acoustic droplet vaporization (ADV). ADV has also been proposed as a possible platform for drug delivery, tumor HIFU (high-intensity focused ultrasound), and phase-change contrast agents.[7–12]

A number of studies have looked at inertial cavitation thresholds for PFC micro- and nano-emulsions.[4,13–15] However, few studies have directly visualized the dynamics during the initial phase change phase or the initial rapid expansion process. Kripfgans *et al.* focused primarily on the dynamics initiating vaporization and characterized the threshold dependence between droplet size and acoustic parameters for ADV.[3] Wong *et al.* experimentally measured the expansion rate of the expanding droplets after vaporization using ultra-high speed imaging.[16] Direct numerical studies related to ADV, carried out by Ye and Bull in 2004 and 2006, looked at the expansion process of bubbles in rigid and flexible channels.[17,18] Qamar *et al.* derived a simplified model including the conversion process from liquid to gaseous DDFP in a numerical model, which matched well with experimental results.[19] Recently, Qamar *et al.* used the earlier simplified model as an initial condition for a full 2D simulation describing bubble expansion in a channel.[20] However, all of the numerical simulations assume that an initial perfectly spherical single bubble nucleus or bubble is formed at the onset of ADV and the bubble remains spherical throughout the first few microseconds. Experimental studies have focused on the events within the first microsecond with nucleation site formation or the expansion process (spanning 600 μs), which may have overlooked important dynamics during the rapid expansion period when stresses are the highest.[3,16,21,22] Recent experiments and simulations performed by Li *et al.*, focusing on the first microsecond after ADV onset, has elucidated a potential mechanism behind the triggering of ADV.[23] It was shown that a dependence between droplet size and wavelength resulted in predicable acoustic wave focusing or interactions determining initial phase change nucleation site formation. In this investigation, the goal was to investigate the dynamics of the early time scale events (<5 μs) and observe the dynamics leading into the transition of a liquid PFC droplet to complete conversion to a gas PFC bubble.

Individual PFC microdroplets (N = 112, mean = 9.1 μm, and STD = 1.2 μm) were isolated at the bottom of an acrylic tank filled with degassed deionized (DI) water maintained at body temperature (37 °C) using a heated recirculating pump (HTP-1500, Adroit Medical Systems, Loudon, TN). The PFC microdroplets featured a DDFP (C_5F_{12}, CAS #: 678–26–2) liquid core and an albumin shell. Details on the formulation of the DDFP microdroplets can be found in Kripfgans *et al.*[1] An inverted microscope (Nikon Eclipse TE2000-S, Nikon, Melville, NY) featuring a 20× objective with 10× internal magnification was used along with an ultra-high speed camera (SIM802, Specialised Imaging Ltd., Hertfordshire, UK) equipped with a 50 mm f/1.4 Nikkor lens reverse mounted to a 70–300 mm Tamron f/4–5.6 macro lens, providing an additional 1.4× to 6× magnification, giving a field of view on the order of 60 × 45 μm^2 (Fig. 1). The ultra-high speed camera was capable of acquiring 16 frames using 8 discreet onboard CCD sensors (1360 × 1024 pixels) with exposures as short as 5 ns and 5 ns between frames. The ADV process was initiated using a single pulse from a 7.5 MHz single element focused (f/2) transducer (37.5 mm diameter Panametrics A321S, Olympus, Waltham, MA) driven by a function generator (HP 3314A) and a pulse amplifier (Ritec GA-2500-A) gated by a second function generator (Aligent 33120A). In order to supply

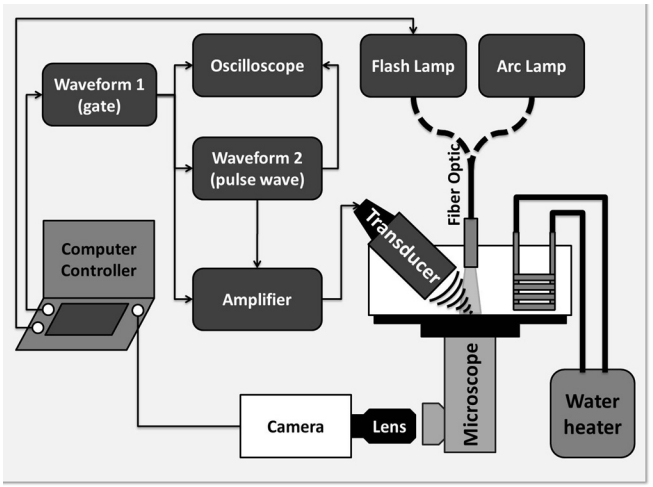

FIG. 1. A schematic of the experimental setup. The transducer was held confocal to the microscope objective using a custom machined bracket. Acoustic pulse length and power was modulated from a HP 3314A function generator. Timing between the transducer, amplifier gate, ultra-high speed camera, and flash lamp was accomplished using a laptop equipped with an external controller running SIM Control (Specialised Imaging Ltd., Hertfordshire, UK).

sufficient light to image the ADV process, the field of view was illuminated using a 300 J flash lamp (Adaptec AD300, Adapt Electronics, Essex, UK) providing 15 μs burst of light.

Approximately 25 μs after the initial triggering of the ultrasound the pressure wave arrived in the field of view initiating the subsequent ADV event (see Figures 2–4). In Figures 2–4 the first frame shows an 8 μm liquid droplet immediately before vaporization. The ADV process begins with the formation of a single gas nucleation site (Figure 2, frame 2) followed by the occasional second nucleus (Figure 3, frame 2) along the axis of propagation for the ultrasound. The generation of two gas nuclei on axis with the propagating ultrasound pulse is consistent with previous experimental observations.[3,16] After nucleation the liquid DDFP continues to convert from liquid to gas phase. Visually,

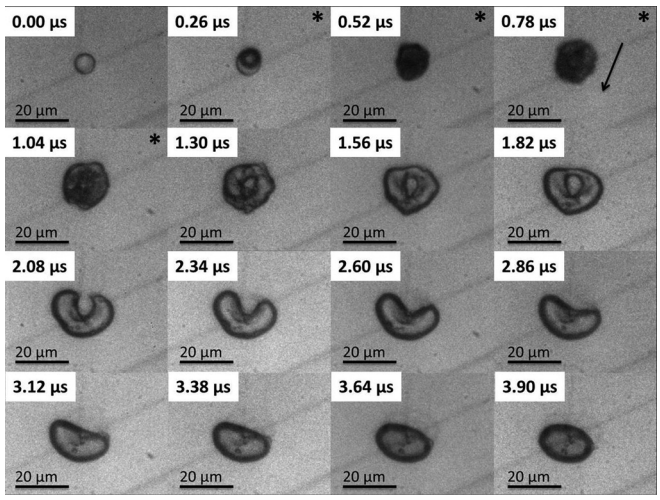

FIG. 2. The image sequence shows an 8.3 μm PFC liquid microdroplet undergoing the ADV process initiated by a single pulse of 8 cycles at 7.5 MHz and 3.6 MPa peak negative pressure. The "*" demarcates the presence of the ultrasound pulse in the field of view, and the arrow indicates the direction of the ultrasound wave. Visually, perforation of the bubble occurs after the initial nucleation and after the ultrasound wave has passed at approximately 1 μs after the initial nucleus is seen.

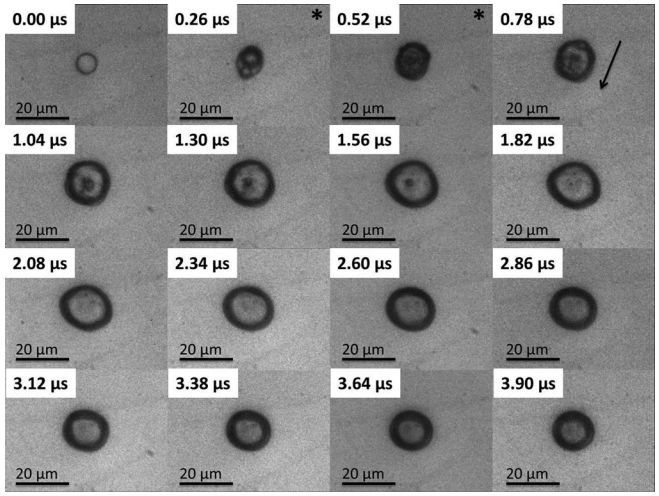

FIG. 3. The image sequence shows an 8.3 μm PFC liquid microdroplet undergoing the ADV process initiated by a single pulse of 4 cycles at 7.5 MHz and 3.6 MPa PNP. The "*" indicates the presence of the ultrasound pulse in the field of view, and the arrow indicates the direction of the ultrasound wave. The reduction in pulse length suppresses the creation of the bubble torus, and the bubble remains largely spherical throughout the early stages of ADV.

complete transition from liquid to gas for the measured droplet population (9.1 $\pm$ 1.2 μm) occurred in under 0.5 μs. Throughout the study, there was no visual indication of external cavitation gas nuclei from the bulk fluid impinging on the microdroplet initiating the ADV process. This suggests that the ADV process as observed here is initiated by dynamics independent from acoustic cavitation of the bulk fluid.

Depending on the acoustic power and the number of cycles, the bubbles immediately after phase change could deform into a bubble torus (Figures 2 and 4). The toroidal bubble was unable to maintain its shape and quickly pinched off at one end of the torus forming a crescent shape (Figure

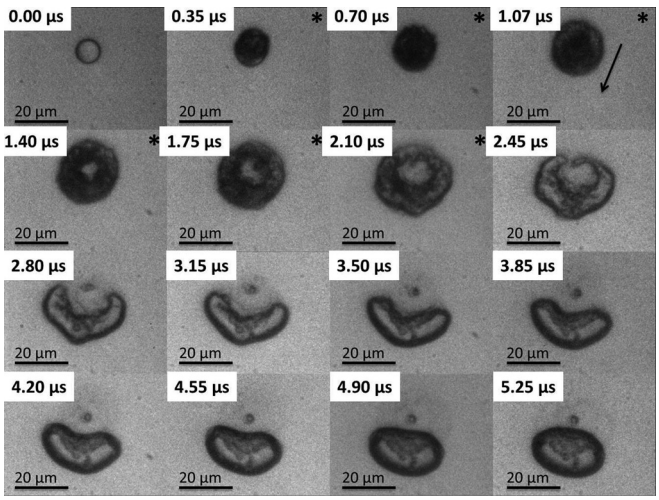

FIG. 4. The image sequence shows an 8.5 μm DDFP liquid microdroplet undergoing the ADV process initiated by a single pulse of 16 cycles at 7.5 MHz and 3.6 MPa PNP. The "*" demarcates the presence of the ultrasound pulse in the field of view, and the arrow indicates the direction of the ultrasound wave. Visually, perforation of the bubble resulting in a bubble torus is seen approximately 1 μs after the initial nucleation. A combination of elevated pulse length and acoustic pressure results in what appears to be a violent ADV process.

2, frame 4) and eventually returning to a spherical configuration. A consistent pinch off of the bubble torus was observed along the upper half of the bubble. This was likely due to the shallow angle of the ultrasound transducer in the tank (25° from horizontal) as well as the propagating direction of the ultrasound (from top to bottom in the images). Typical lifetime of the bubble torus prior to pinch off is on the order of 1–1.5 μs with the initial formation of the torus at 1 μs after nucleation. Formation of the torus did not always coincide with the presence of the ultrasound wave (Figure 2), suggesting that the dynamics are likely due to residual fluid inertia generated from ultrasound bubble interactions. Similar dynamics have been previously observed, which includes microjets from cavitation events near boundaries.[24–27] However, unlike inertial cavitation, the bubble does not fully collapse, and no rebound events were observed. This could be due to the high internal pressure seen in the PFC gas bubble immediately after phase change resisting collapse from the acoustic pressure. Using the ideal gas law, given that liquid DDFP has a density of 1630 kg/m^3 and a molar mass of 288 g/mole,[1,28] it can be estimated that if a 9 μm diameter liquid DDFP microdroplet is instantaneously converted to a gas bubble with no change in size, the instantaneous internal gas pressure will be on the order of 14.32 MPa. As the droplet converts to the gas phase and begins to expand, it is known that the expansion process is heavily influenced by both interfacial tension and fluid viscosity.[17,19] With increasing bulk fluid viscosity, one can anticipate increased damping and an increased acoustic pressure threshold to drive the bubble and develop the fluid inertia to collapse the bubble. As the bubble rapidly expands to reach equilibrium with the surrounding ambient fluid pressure, a corresponding decrease in bubble internal pressure is also occurring. Conceivably, by increasing acoustic pressure and/or pulse length, a combination of acoustic pressure and increased fluid inertia is likely to overpower the decreasing internal bubble pressure resulting in an increased likelihood for bubble torus formation. The resistance to deformation of the bubble interface is dependent on the interfacial tension between the bubble and the bulk fluid. Selection of droplet shell properties to decrease or increase surface tension or shell elasticity can result in a decrease or increase in threshold for toroidal bubble formation. Once again using the ideal gas law, it can be shown that a 9 μm diameter droplet will result in an approximately 45 μm diameter bubble. For such a bubble the resonant frequency is on the order of 145 kHz; therefore, it is unlikely that the formation of the torus is due to a bubble resonance.[29] However, the interaction of the field with the gas nuclei is closer to resonance size but with a correspondingly higher internal gas pressure.

The likelihood of collapsing a bubble by creating an invagination to form a toroidal bubble can be modulated by reducing the number of cycles (thus reducing pulse duration) or the acoustic pressure (Figure 5). By reducing the pulse duration to 4 cycles, the droplet was still able to undergo the ADV process, and the possibility of forming the torus was completely avoided regardless of the pressures tested (2.2–5.1 MPa peak negative pressure). Maintaining a low acoustic pressure and varying the pulse length was less effective at mitigating chances of collapsing the bubble. At

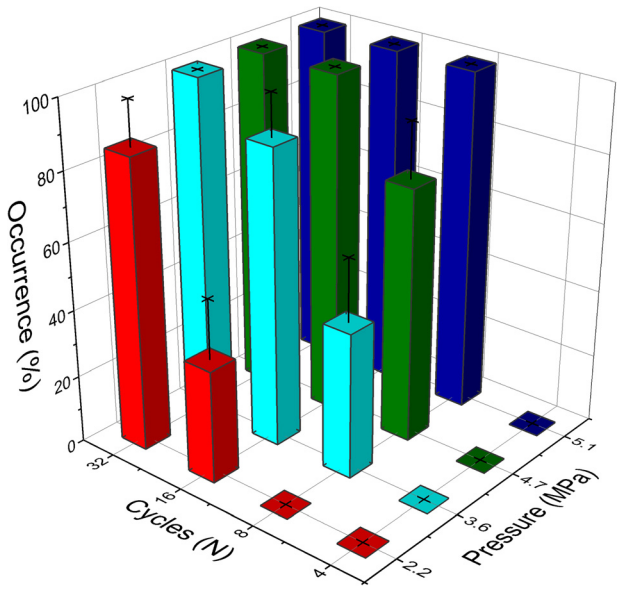

FIG. 5. Rate of occurrence observed in bubble torus formation as a function of number of inputted cycles and PNP for droplets of 9.1 μm (STD = 1.2 μm) droplets vaporized using single pulses from a 7.5 MHz transducer.

2.2 MPa, 4 and 8 cycles were sufficient to vaporize the droplets while avoiding the collapse; however, the incidence rate of collapse was greatly increased after 16 cycles. The elevated chances of generating a bubble torus could be from the first several cycles inducing nucleation and phase change over the course of one microsecond (approximately 8 cycles at 7.5 MHz) and later cycles in the longer pulse lengths interacting with the gaseous bubble allowing for collapse.

The conditions necessary to vaporize DDFP microdroplets and collapse the bubble to create a temporary bubble torus at 7.5 MHz were observed. Modulation of acoustic pressure and pulse length allowed for control over the formation of a transient bubble torus. Elevated pulse length or acoustic pressure would lead to eventual torus formation. Associated stresses from invagination of the bubble may lead to potential tissue damage similar to that seen in liquid microjets formed from HIFU bubble collapse.[25,27] Furthermore, the final pinch off of the bubble torus reforming leading to eventual reformation to a spherical bubble may also generate high stresses near the endothelium. Such cellular damage has been observed in liquid plug ruptures in the lung airway models may result in sufficiently high stresses leading to epithelial lung damage.[30] However, sufficiently short pulse lengths eliminated the possibility of creating a transient bubble torus over the range of acoustic pressures tested. Additionally it was confirmed that, for the appropriate conditions, single nucleation sites can be formed, and the evolution of the expanding bubbles even within the first 10 μs remain largely spherical. This suggests that previous assumptions in computational models are reasonable if acoustic pulses used are low intensity and sufficiently short. The perturbation leading to the temporary formation of a bubble torus could be due to fluid inertial or from acoustic radiation force.

This research was funded by NIH grants (Nos. R01EB006476 and S10 RR022425).

[1]O. D. Kripfgans, J. B. Fowlkes, D. L. Miller, O. P. Eldevik, and P. L. Carson, Ultrasound Med. Biol. **26**, 1177 (2000).
[2]J. L. Bull, Crit. Rev. Biomed. Eng. **33**, 299 (2005).
[3]O. D. Kripfgans, M. L. Fabiilli, P. L. Carson, and J. B. Fowlkes, J. Acoust. Soc. Am. **116**, 272 (2004).
[4]T. Giesecke and K. Hynynen, Ultrasound Med. Biol. **29**, 1359 (2003).
[5]O. D. Kripfgans, C. M. Orifici, P. L. Carson, K. A. Ives, O. P. Eldevik, and B. J. Fowlkes, IEEE Trans. Ultrason. Ferroelctr. Freq. Controll **52**, 1101 (2005).
[6]M. Zhang, M. L. Fabiilli, K. J. Haworth, J. B. Fowlkes, O. D. Kripfgans, W. W. Roberts, K. A. Ives, and P. L. Carson, Ultrasound Med. Biol. **36**, 1691 (2010).
[7]M. L. Fabiilli, J. A. Lee, O. D. Kripfgans, P. L. Carson, and J. B. Fowlkes, Pharmaceut. Res. **27**, 2753 (2010).
[8]M. L. Fabiilli, K. J. Haworth, I. E. Sebastian, O. D. Kripfgans, P. L. Carson, and J. B. Fowlkes, Ultrasound Med. Biol. **36**, 1364 (2010).
[9]P. S. Sheeran and P. A. Dayton, Curr. Pharm. Design **18**, 2152 (2012).
[10]N. Rapoport, A. M. Kennedy, J. E. Shea, C. L. Scaife, and K. H. Nam, J. Control. Release **153**, 4 (2011).
[11]N. Reznik, R. Williams, and P. N. Burns, Ultrasound Med. Biol. **37**, 1271 (2011).
[12]P. Zhang and T. Porter, Ultrasound Med. Biol. **36**, 1856 (2010).
[13]M. L. Fabiilli, K. J. Haworth, N. H. Fakhri, O. D. Kripfgans, P. L. Carson, and J. B. Fowlkes, IEEE Trans. Ultrason. Ferrelctr. Freq. Controll **56**, 1006 (2009).
[14]A. H. Lo, O. D. Kripfgans, P. L. Carson, E. D. Rothman, and J. B. Fowlkes, IEEE Trans. Ultrason. Ferrolectr. Freq. Controll **54**, 933 (2007).
[15]E. Sassaroli and K. Hynynen, Ultrasound Med. Biol. **33**, 1651 (2007).
[16]Z. Z. Wong, O. D. Kripfgans, A. Qamar, J. B. Fowlkes, and J. L. Bull, Soft Matter **7**, 4009 (2011).
[17]T. Ye and J. L. Bull, J. Biomech. Eng. **126**, 745 (2004).
[18]T. Ye and J. L. Bull, J. Biomech. Eng. **128**, 554 (2006).
[19]A. Qamar, Z. Z. Wong, J. B. Fowlkes, and J. L. Bull, Appl. Phys. Lett. **96**, 143702 (2010).
[20]A. Qamar, Z. Z. Wong, J. B. Fowlkes, and J. L. Bull, J. Biomech. Eng. **134**, 031010 (2012).
[21]O. Shpak, T. Kokhuis, Y. Luan, D. Lohse, N. de Jong, B. Fowlkes, M. Fabiilli, and M. Versluis, J. Acoust. Soc. Am. **134**, 1610 (2013).
[22]O. Shpak, L. Stricker, M. Versluis, and D. Lohse, Phys. Med. Biol. **58**, 2523 (2013).
[23]D. S. Li., O. D. Kripfgans, M. L. Fabiilli, J. B. Fowlkes, and J. L. Bull, "Initial Nucleation Site Formation Due to Acoustic Droplet Vaporization," Appl. Phys. Lett. (to be published).
[24]W. Lauterborn and C.-D. Ohl, Ultrason. Sonochem. **4**, 65 (1997).
[25]T. Kodama and Y. Tomita, Appl. Phys. B **70**, 139 (2000).
[26]O. Lindau and W. Lauterborn, J. Fluid Mech. **479**, 327 (2003).
[27]H. Chen, X. Li, M. Wan, and S. Wang, Ultrasonics **49**, 289 (2009).
[28]T. M. Reed, in *Fluorine Chemistry*, edited by J. H. Simons (Academic Press, 1964), Vol. 5.
[29]C. E. Brennen, *Cavitation and Bubble Dynamics* (Oxford University Press, 1995).
[30]D. Huh, H. Fujioka, N. Tung, R. Paine III, J. B. Grotberg, and T. Shuichi, Proc. Natl. Acad. Sci. U.S.A. **104**, 18886 (2007).